of the back-pressure ahead of shock front 1 which determined by it.

The author thanks V. K. Kedrinskii for his discussion of the paper.

LITERATURE CITED

1. N. L. Coleburn and L. A. Roslund, "Interaction of spherical shock waves in water," in: Fifth International Symposium on Detonation, Pasadena, California, August 18-21 (1970), pp. 581-588.
2. F. A. Baum, L. P. Orlenko, K. P. Stanyukovich, V. P. Chernyshev, and V. I. Shekhter, Physics of Explosion [in Russian], Nauka, Moscow (1975).
3. B. V. Zamyshlyaev and Yu. S. Yakovlev, Dynamic Stresses from an Underwater Explosion [in Russian], Sudostroenie, Leningrad (1967).
4. M. A. Tsikulin, "Overtaking of a single triangular pressure profile by another in the asymptotics of shock waves," Zh. Prikl. Mekh. Tekh. Fiz., No. 2 (1960).

PHASE TRANSITIONS IN SHOCK WAVES (REVIEW)

L. V. Al'tshuler

UDC 536.424

INTRODUCTION

The propagation of shock waves in a number of solids is accompanied by polymorphic transitions which change their atomic structure. The formation of new crystalline modifications in a short time of the order of 10 μsec is one of the most interesting problems in the physics of shock waves and high pressures. Dynamic recrystallization processes are extensively used in practice, e.g., in machine-building technology, for strengthening components, and for obtaining metastable high-pressure phases.

Phase transitions propagating in a metal at the detonation velocity were first detected in iron [1]. By now, polymorphic transitions in shock waves have been recorded in many metals, semiconductors, oxides, and almost all minerals and rocks. The characteristics of a few typical transitions, investigated under both dynamic and static conditions, are given in Table 1, where σ_{HYP} is the Hugoniot yield point, σ_1 is the transition stress from dynamic measurements, and p_1 is the transition pressure from static measurements (all quantities are in kilobars).

The problem of phase transitions in shock waves has various aspects. The thermodynamic analysis is based on the limiting parameters of the steady-state regimes of propagation of the shock waves. The set of stationary states determines the Hugoniot adiabat of the compressed medium. The intersection with the phase boundaries causes a break in the adiabats and under certain conditions can lead to decay of the shock front and formation of two-wave configurations from the advancing waves and the slower transition waves. A knowledge of the kinetics of the transitions is particularly important for obtaining a realistic picture of the phenomenon; transitions of martensite type have a number of special features and proceed in compression and discharge wave fronts in accordance with specific mechanisms of low-temperature recrystallization.

1. Hugoniot Adiabat in the Phase Plane

1.1. Phase-Transition Criterion. The effect of melting and polymorphic transitions on the configuration of the Hugoniot adiabat was investigated in [8-13]; the results from these studies are partially discussed in the review [14].

The thermodynamic characteristics of the medium change discontinuously at the boundary between the single-phase region and the region of existence of phase-mixture equilibrium. As a result, the shock-compression adiabat undergoes a discontinuous change on intersecting

Moscow. Translated from Zhurnal Prikladnoi Mekhaniki i Tekhnicheskoi Fiziki, No. 4, pp. 93-103, July-August, 1978. Original article submitted June 6, 1977.

 0021-8944/78/1904-0496$07.50

the phase boundary. The direction of deflection of the adiabat (Fig. 1a) is given by the equation [9]

$$\operatorname{sgn}\Delta = \operatorname{sgn} Q\left[dT/dp - (\partial T/\partial p)_{S1}\right],\ \Delta = (\partial V/\partial p)_{\Gamma+} - (\partial V/\partial p)_{\Gamma-}, \tag{1.1.1}$$

where the derivatives $(\partial V/\partial p)_{\Gamma+}$ and $(\partial V/\partial p)_{\Gamma-}$ are taken along the dynamic adiabat above and below the point of discontinuity; $(\partial T/\partial p)_{S1}$ is the derivative of the first phase; dT/dp is the derivative of the phase boundary; and Q is the latent heat of phase transition.

For further analysis, the Hugoniot equation $H - H_c = (1/2)(p - p_c)(V + V_c)$ is written in differential form [8, 12, 13], relating $(\partial V/\partial p)_\Gamma$ with $(\partial V/\partial p)_S$ and the slope $m^2 = (p - p_c)/(V_c - V)$ of the Rayleigh–Michelson line (Fig. 1b) (here and above, p_c and V_c are the state parameters ahead of the wave front). The required differential equation is obtained with the use of the identity

$$(\partial H/\partial p)_\Gamma - V = T(\partial p/\partial T)_S[(\partial V/\partial p)_\Gamma - (\partial V/\partial p)_S];$$

substituting the relationship

$$(\partial H/\partial p)_\Gamma - V = (1/2)(p - p_c)[(\partial V/\partial p)_\Gamma + m^{-2}],$$

we obtain

$$\left(\frac{\partial V}{\partial p}\right)_\Gamma = -m^{-2} + \frac{m^{-2} + \left(\frac{\partial V}{\partial p}\right)_S}{1 - \frac{p - p_c}{2T}\left(\frac{\partial T}{\partial p}\right)_S}. \tag{1.1.2}$$

The discontinuity in the adiabat occurs because of the different values of the isoentropic derivatives on the two sides of the phase boundary. Compared to the adjoining single-phase states (subscript 1) the compressibility of the phase mixture (subscript φ) changes by the amount [11, 14]

$$(\partial V/\partial p)_{S\varphi} - (\partial V/\partial p)_{S1} = -(c_{p1}/T)[dT/dp - (\partial T/\partial p)_{S1}]^2. \tag{1.1.3}$$

As regards the derivative $(\partial T/\partial p)_{S1}$, in p – T coordinates all thermodynamic processes occurring in the two-phase region are described by the equilibrium line. Therefore,

$$(\partial T/\partial p)_{S\varphi} - (\partial T/\partial p)_{S1} = dT/dp - (\partial T/\partial p)_{S1}. \tag{1.1.4}$$

As is well known [15], the wave front loses stability if at any point the slope of the adiabat becomes smaller than the slope of the wave ray [if $(\partial V/\partial p)_\Gamma < -m^{-2}$]. An instability of this type can appear when the second term in the right-hand side of (1.1.2) becomes negative due to large compressibility of the phase mixture. According to (1.1.2) and (1.1.3), the criterion for the stability loss is the inequality

$$(c_{p1}/T)[dT/dp - (\partial T/\partial p)_{S1}]^2 > m^{-2} + (\partial V/\partial p)_{S1}. \tag{1.1.5}$$

For obtaining some estimates it is convenient to introduce the volume expansion coefficient $\alpha_1 = (c_{p_1}/VT)(\partial T/\partial p)_{S1}$, the wave velocity D, and the speed of sound c_1. Then inequality (1.1.5) can be rewritten in the following form:

$$\left[\sqrt{\frac{c_{p1}}{T}}\frac{dT}{dp} - \sqrt{\frac{T}{c_{p1}}}V_1\alpha_1\right]^2 > \frac{V_c^2}{D^2} - \frac{V^2}{c_1^2}.$$

A different situation occurs if the values of dT/dp and $(\partial T/\partial p)$ are close and therefore the wave retains stability. In this case, the increase in the compressibility [as in (1.1.3)] can be neglected as the square of a small quantity and only the change in the quantity $(\partial T/\partial p)_S$ [as in (1.1.4)] need be taken into consideration.

1.2. Classification of Phase Transitions and Adiabat Configuration. The classification of phase transitions developed in [12, 13] is based on different variants of arrangements of the phase boundary in relation to the isotherms and isoentropic lines of the low-pressure phase. In p – T coordinates the equilibrium line is characterized by the derivatives

$$dT/dp = (T/Q)(V_2 - V_1),$$
$$dS_1/dp = (c_{p1}/T)[dT/dp - (\partial T/\partial p)_{S1}].$$

With the use of the identities

$$dV_1/dp = (dV/dp)_T + (\partial V_1/\partial T)_{p1}dT/dp, \tag{1.2.1}$$

$$\frac{dS_i}{dp} = \frac{c_{pi}}{T}\left(\frac{\partial V_i}{\partial T}\right)_{pi}^{-1}\left[\frac{dV_i}{dp} - \left(\frac{\partial V_i}{\partial p}\right)_{Si}\right] \qquad (1.2.2)$$

the values of these derivatives determine the slopes of the dV_i/dp boundaries in p — V coordinates.

The basis of the classification is provided by different combinations of the signs of dT/dp and dS_i/dp, presented in the left part of Table 2, together with possible [12] combinations of the signs of $\Delta V = V_2 - V_1$ and Q. The orientations of the phase boundaries on p — V diagrams determined from (1.2.1) and (1.2.2) and the signs of deflections of the adiabats as given by (1.1.1) are shown in the right part of Table 2. For the first type of transition, in p — V variables the phase boundary has a milder slope than the isotherms of the first phase, for the second type, it is steeper than the isoentropic lines; and for the third type, the slope of the boundary is greater than that of the isotherms and smaller than that of the isoentropic lines.

We first consider phase transitions of the second and third types accompanied by a volume increase, i.e., normal melting of solid substances (see Table 2). Here inequality (1.1.5) is not satisfied, the shock wave remains stable, and the formation of the liquid phase occurs over the thickness of the front of a single surface discontinuity [16]. The possible configurations of the adiabats for $\partial S_i/\partial p < 0$ and $\partial S_i/\partial p > 0$ are depicted in Fig. 2, where the symbols Sol and L denote the regions of solid and liquid state, respectively. In the first case (Fig. 2a), in intersecting the boundary of the two-phase region, the adiabat is deflected to the left ($\Delta < 0$); in the second case (Fig. 2b), it is deflected to the right ($\Delta > 0$). In metals and ionic compounds $dS_i/dp|_{p=0} < 0$ [13]. Perhaps this situation persists even at high pressures. What happens in reality is still unknown, since as a rule, discontinuities of the adiabat for the parameters of melting have not been detected in a large number of measurements of the dynamic compressibility of elements and chemical compounds. Therefore, it may be assumed that for the investigated substances the melting curves are very similar to the isoentropic lines of the solid phase. Apparently, sulfur is the only known exception [17]. The sharp increase of the slope of its adiabat shows that this transition, belongs to the second type.

On increasing the pressure, all polymorphic transitions occur with a volume decrease. Denser phases are formed also during solidification of normal liquids and anomalous melting. For the transitions of the first type, the schematic pattern of intersection of the two-phase region by the shock-compression curve is shown in Fig. 3. Examples of such transitions are Fe$\alpha \rightarrow$ Feε and the melting of bismuth. The polymorphic transitions α-quartz—stishovite, graphite—diamond, and boron nitride—borazon belong to the second type (Fig. 4). As regards solidification of liquids, it may not even occur during shock compression, if the adiabat does not intersect the phase boundary [9].

As a rule, the formation of high-pressure dense phases leads to a decay of the shock front. The dynamic compression curve (Fig. 5a) for two-wave configurations contains singular points 1, 2, and 3, which divide it into four branches: adiabat of the first phase with initial state p_0, V_0; adiabat of the double compression of the phase mixture centered at p_1, V_1; and adiabat of the second phase with centers at p_1, V_1 at pressures lower than p_3 and p_0, V_0 at pressures larger than p_3. The last discontinuity, with the disappearance of the two-wave configuration at point 3, is caused [18, 10] by the change in the nature of compression from double to single. Analytically, the transition to different Hugoniot adiabats is interpreted through the substitution of the corresponding values of $(\partial V/\partial p)_S$, $(\partial T/\partial p)_S$, and p_c into Eq. (1.1.2).

The adiabat of the single (one-wave) compression is very similar to the curve investigated above and can be formally constructed even for the instability range $p_1 < p < p_3$. The states on this adiabat satisfy the three conservation laws and also the condition of overall (relative to p_0, V_0) entropy increase if they do not lie too close to the lower boundary of the interval. Nevertheless, a direct transition of the type OC is not realized in practice due to the gas-dynamic instability and breakdown of the second law of thermodynamics. Actually, single-wave transition OC is equivalent to three individual discontinuities between the equilibrium states O, A, B, and C moving with the same speed. Of these, the first and third increase the entropy of the medium, whereas the intermediate discontinuity AB, containing the segment of the adiabat with negative mean curvature, decreases the entropy and is

TABLE 1

Material	σ_{HYP}	σ_1	p_1
Fe	10±3	129±2 [2]	118—133
KCl	0,7±0,3	21±0.2 [3]	20±0,5
Fe_3O_4	~10	216±15 [4]	250±15
Si	45±5	105±6 [5, 6]	104—140
Ge	42±3	142±3 [5, 7]	120—125
GaAs	84±8	203±11 [4]	175—185

TABLE 2

Type of transition	$\frac{dT}{dp}$	$\frac{dS_1}{dp}$	ΔV	Q	$\frac{dV_1}{dp}$	Δ	Remark
1	<0	<0	<0	>0	$<\left(\frac{\partial V}{\partial p}\right)_{T_1}$	<0	Polymorphic transition; anomalous melting
2	>0	>0	<0 >0	<0 >0	$>\left(\frac{\partial V}{\partial p}\right)_{S_1}$	<0 >0	Polymorphic transition; solidification
3	>0	<0	>0	>0	$>\left(\frac{\partial V}{\partial p}\right)_{T_1}$; $<\left(\frac{\partial V}{\partial p}\right)_{S_1}$	<0	Melting

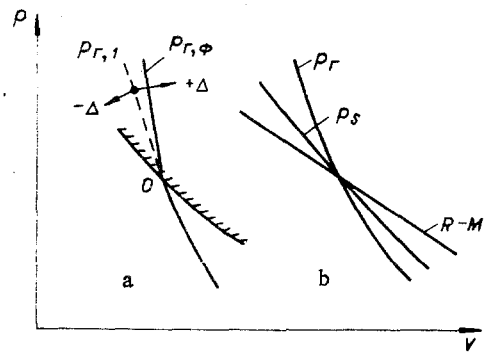

Fig. 1

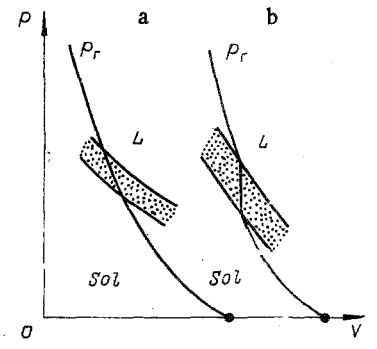

Fig. 2

therefore unstable. The proposed concept of Bethe instability is the most rigorous, since the discussion of the discontinuity as an integral [19] decrease of entropy on an individual segment of the front does not contradict [15] the second law of thermodynamics.

2. Kinetics of Crystallization in Shock Waves

The information on the kinetics of transitions in shock waves has been obtained primarily from the study of plane shock pulses. Therefore, we consider the formation of shock pulses in the simplest representation [20, 18], i.e., formed by the impact of a plate of finite thickness on the substance undergoing the phase transition. For a given velocity of impact on the collision surface, states that lie on the retardation curve C_1C of the striker appear (see Fig. 5a). The instantaneous response of the medium is its compression along the metastable state of the first phase up to pressure C_1. Subsequent transitions lead to a pressure decrease in the wave front, i.e., along the metastable adiabat of the first phase in the layers behind the front and on the collision surface, i.e., along the retardation curve CC_1. On the p—V diagram the set of states forms an evolutionary trajectory which approaches the wave ray 1—C asymptotically. The two-wave profile of the wave thus formed is schematically shown in Fig. 5b together with the discharge shock wave [15, 18].

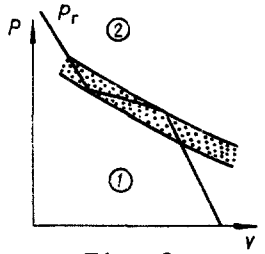

Fig. 3

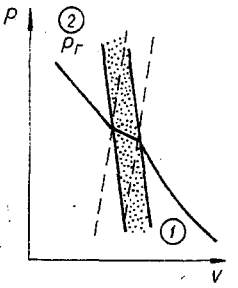

Fig. 4

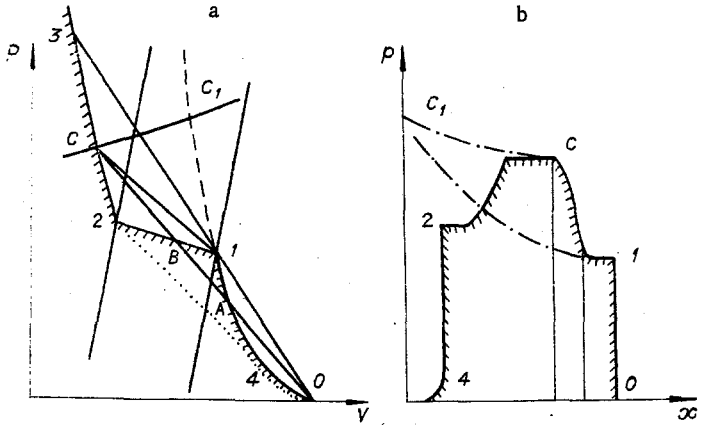

Fig. 5

A mathematical description of the disintegration of the front requires numerical computations based on some idealized scheme of the phenomenon. An appropriate theory of the problem has been developed in [21-25]. The simplest model is the hydrodynamic single-velocity model, which assumes the equality of pressures, temperatures, and velocities for the particles of both phases. In carrying out the computations, the equations of motion are closed by the equations of state of the two phases and the expression for the rate of transition

$$df/dt = (f_{eq} - f)/t_{ch}, \qquad (2.1)$$

where f is the concentration of the second phase, f_{eq} is its equilibrium concentration, and t_{ch} is the characteristic time of transformation. If the velocity of the first plastic wave is close to the acoustic velocity, then its amplitude along the path of propagation undergoes exponential attenuation:

$$p(x) = p_1 + (p_{c_1} - p_1)\exp(-x/(2Dt_{ch})),$$

where p_{c_1} is the applied pressure and p_1 is the transition pressure (see Fig. 5a).

According to the representations discussed above, the start and termination of the formation of the new phase occur at the equilibrium transition pressures, and the attenuation of the first plastic wave, the width of the second wave, and the relaxation of the stresses at the collision surface are governed by a single characteristic time of transformation t_{ch}. On a first impression, the experimental results support such simplified treatment. The pressure profiles recorded by manganin sensors in [26], devoted to the study of phase transitions in iron, are shown in Fig. 6. These experimental curves show the formation of the transition wave and the discharge shock wave appearing during reverse recrystallization. Similar results have been obtained in the study of potassium [27, 28], silicon, and germanium [15] halegonides by the magnetoelectric technique [18].

Let us ascertain how closely the transition pressures recorded under dynamic and static conditions coincide. For a correct comparison it is necessary to consider the anisotropy of the one-dimensional compression in the shock wave, which is related to the hardness. According to the elastoplastic model, the measured stresses in the shock wave exceed the hydrostatic pressures by two-thirds of the dynamic yield point Y. For the Poisson coefficient ν =

0.33, this amount is equal to three times the Hugoniot elasticity limit σ_{HYP} [18, 25]. This approach is not valid for all materials. Experiments with sapphire [29] and tungsten [30] show that here a catastrophic loss of hardness occurs above the elasticity limit and (as a consequence) the dynamic recordings are superposed on the hydrostatic adiabats. In spite of some ambiguity in the interpretation, the data presented in Table 1 indicate that the transition pressures almost coincide under static and dynamic conditions. This agreement is found in iron, potassium chloride, magnetite, silicon, and (after correcting for hardness) in germanium and GaAs. An exception to this general rule is quartz, in which the transition pressure in the shock wave coincides with the Hugoniot elasticity limit and exceeds the equilibrium pressure [31].

We now turn to the kinetic characteristics of the transitions in shock waves. For iron, the most accurate results have been recently obtained in [2] with the use of laser interferometry on samples of variable thickness. The characteristic time of transition, computed from the attenuation of the first wave for different impact pressures, is 0.16 μsec. It by far exceeds the time scale of the transition wave (0.05 μsec) recorded in the same experiments. "The detected contradiction shows that the model assuming a single constant relaxation time is too simplified" [2]. Perhaps the initial, purely thermodynamical interpretation of the phenomenon is far from reality.

Interesting kinetic characteristics of transition are detected in the study of the phase transition in potassium halogenides [28, 3, 16]. Recording the bulk velocity profiles during dynamic compression and discharge, the authors of [28] show the dependence of the transition time in the second plastic wave on its amplitude ($t_{ch} \approx 0.4$-0.6 μsec for 28 and 0.2 μsec at 38 kbar) and the incompleteness of the phase transition behind its front. The high- and low-pressure phase mixture formed here is represented in Fig. 7 by the metastable adiabat 1—2 merging into the adiabat of the second phase at pressures p_2 much larger than the equilibrium pressure. A strong hysteresis of the reverse recrystallization in the discharge wave is also established in [28]. The start of the process (point 3) coincides with the formation of the rarefaction shock wave and occurs at pressures differing from the equilibrium pressure by a factor of two (10 kbar instead of 20 kbar). Subsequently [3], these results were supplemented by the measurements of the relaxation of the pressures at the collision surface. The first stage of transition occurring "instantaneously" led to states of the same metastable adiabat of the phase mixture (see Fig. 7). The completion of the process occurred with measurable velocities that were different for different crystallographic directions. At pressures an order of magnitude higher than the equilibrium pressure, the transition times in potassium halogenides were estimated [16] optically from the reflectivity of the front. The two-wave configuration does not appear at such pressures and the formation of the dense phase occurs over the thickness of the single compression wave front for a period smaller than 10^{-12} sec.

Many of the above-mentioned characteristics are typical not only for potassium halogenides. The incompleteness of the transitions at large residual pressures occurs in boron nitride [28], iron [2], quartz [33, 31], and graphite [33]. In quartz and graphite [34], the metastable adiabats of the mixture coincide remarkably with the critical wave ray 1—3 of Fig. 5a. The hysteresis in the reverse recrystallization is clearly seen in iron (see Fig. 6). Its existence makes it possible to synthesize diamond and borazon in storage ampules.

3. Mechanisms of Phase Transitions in Shock Waves

As shown by the results of Sec. 2, the recrystallization in shock waves obeys specific and mainly nonthermodynamic rules. This fact was given attention in the mid-1960's in a number of investigations, in particular [35, 36].

The specific features of polymorphic transitions in dynamic pulses is naturally explained by the basic generality of the mechanism of deformation and transition and by the special characteristics of shock discontinuities. "For sufficiently large pressure gradients the shock front may be compared with a mill, which crushes the noncompacted material in its forward part and then transfers the atoms of high-density region into states that are stable under these conditions" [35]. The asymmetry of the transitions during the application and removal of the pulsed loads is related to the effect of the shock front on the substructure of the medium. The reverse recrystallization occurs during monotonic pressure decrease in the isoentropic discharge wave. On the other hand, the formation of the high-pressure phase is preceded by the passage of the first plastic wave. Its shock front is a surface on which

Fig. 6

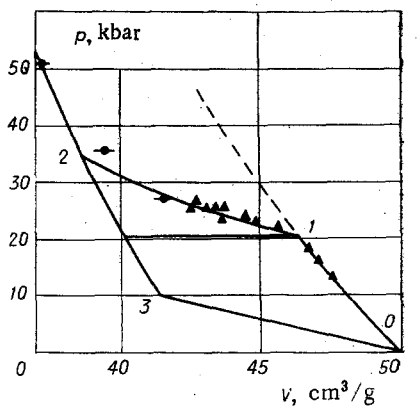

Fig. 7

point, linear, and two-dimensional defects, which become crystallization centers at supercritical pressures, are produced in abundance. Apparently, the phase transitions in shock waves are always similar in type to martensite transitions. The rapid transition of one type of lattice into another is facilitated by nondiffusion martensite rearrangements; they are based on the cooperative motion of many atoms to small distances.

Typical martensite structures are observed in iron and ferrous alloys in the presence of dual recrystallization, $\alpha-\varepsilon-\alpha$. Samples preserved after shock compression have structures containing stacks of fine sheets doubly correlated to the lattice of the initial phase. According to [37], in $\alpha-\varepsilon$ transitions only one variant of orientation is realized for each habit plane, which results in a coherent crystallization of the ε phase. The reverse transition in the same habit plane $(112)_\alpha$ restores the original orientation of the α-phase crystals. Some definite orientation relationships of martensite type are detected [38] in the shock-wave formation of the ω-phase of titanium.

The most direct information is obtained in [39], where the transition of a boron nitride monocrystal into a monocrystal of borazon wurtzite is recorded using pulsed x-ray analysis. Here the thickness of the wave front perhaps covers several lattice periods. It is interesting to note that the cubic structure of zinc blende is the stable phase of high pressure. However, from the point of view of crystal geometry, martensite transition from the original hexagonal structure into hexagonal wurtzite has priority. Similar arguments developed in [32] explain why in a shock wave quartz at once goes over into stishovite, omitting the intermediate coesite phase. "The transition into coesite requires transition of 46 quartz cells into 3 coesite cells. Here the role of final reshuffling of the molecules, which is essentially a nondiffusion process, increases sharply."

The theory of martensite transitions [40-42] was initially developed for coherent phase transitions occurring at atmospheric pressure under the influence of rapid temperature changes. However, the basic rules and results of the theory are equally applicable also to polymorphic transitions in shock waves and discharge waves.

According to the established ideas, nuclei (embryos) present in the initial phase under subcritical conditions are the centers of crystallization of martensite. Therefore, nuclei are present in some quantity in the uncompressed material and are formed as dislocations [35], twins [43], or packing defects in the front of the first plastic wave. For materials in which the phase-transition pressure coincides with the yield point (quartz), the development of the crystallization centers and high-pressure phase occurs simultaneously and autocatalytically.

The activation of the nuclei, i.e., their transition into active centers of crystallization of the new phase, occurs at a nonequilibrium pressure, when the chemical ponderomotive force balances the surface energy of the nucleus and the deformation energy of the crystal matrix surrounding it. The largest nuclei are activated first. The martensite points of direct (p_{1d}) and reverse (p_{1r}) transition during loading and discharge determine the deviations from the thermodynamic equilibrium required for this purpose. The true equilibrium pressure lies between these limits, perhaps nearer to the upper limit. For iron [2], p_{1d} = 130 kbar and p_{1r} = 98 kbar.

The number of active centers of crystallization increases with the deviation from thermodynamic equilibrium. As a result of self-braking processes, which are not yet completely clear, the martensite crystals thus formed have limiting dimensions that are characteristic of each substance. Therefore, very definite concentrations $f_m(p)$ of the new phases, depend only on the number of active centers and determine the positions of the metastable adiabats $p_{\Gamma m}$ of incomplete transition during loading and discharge, correspond to nonequilibrium pressures.

The athermal kinetics of the martensite transition is determined by the number of centers and the rate of linear growth of martensite crystals. The latter equals the velocity of spiral dislocations [4] under the action of shear stresses $\tau \sim (G - G_i)/\gamma \approx (p - p_i)/\gamma$, where G_i and p_i are, respectively, the Gibson potential and pressure required for the activation of a nucleus of radius r_i; γ is the shear deformation of the lattice transition. According to the estimates obtained for carbon steel [44], the transition periods of single grains are 10^{-6}-10^{-7} sec, which in terms of time scales coincide with the transition periods in shock waves.

In a number of materials, rapid athermal transitions occur simultaneously with slower athermal processes of growth of the new phase due to thermally activated formation of crystallization centers. Similar phenomena of two-stage transition occur during dynamic loading of monocrystals of potassium chloride [3].

The present concepts of the mechanisms of martensite transitions may serve as a good babase for the future development of the theory of transitions in shock waves. Such a theory must of necessity include a large number of empirical data on the position of martensite points, metastable adiabats [or $f_m(p)$], and two relaxation times (in general, pressure dependent) — t_a for the athermal process and t_t for the thermally activated process. Athermal kinetics dominates at the first stage and is governed by the equation

$$df/dt = (f_m(p) - f)/t_a \quad (0 < f < f_m(p)),$$

while thermally activated transition occurring at the rate

$$df/dt = (1 - f)/t_t \quad (f_m < f < 1)$$

dominates at the second stage.

Further understanding of transition mechanisms requires new experimental and theoretical investigations. These investigations may, in particular, elucidate the extent to which local heating of materials in the zones of intense slip [29, 30, 45, 46] influences the kinetics of formation.

The author is grateful to E. A. Dynin, O. N. Breusov, and N. M. Kuznetsov for helpful discussions.

LITERATURE CITED

1. B. Bancroft, E. L. Peterson, and S. Minshall, "Polymorphism of iron at high pressure," J. Appl. Phys., 27, No. 3 (1957).
2. L. M. Barker and R. E. Hollenbach, "Shock wave study of the α-phase transition in iron," J. Appl. Phys., 45, No. 11 (1974).
3. D. B. Hayes, "Polymorphic phase transformation rates in shock-loaded potassium chloride," J. Appl. Phys., 45, No. 3 (1974).
4. T. Goto, Y. Syono, I. Nakai, and Y. Nakagawa, "Pressure-induced phase transition in GaAs under shock compression," Solid State Commun., 18 (1976).
5. M. N. Pavlovskii, "Formation of metallic modifications of germanium and silicon under shock-compression conditions," Fiz. Tverd. Tela, 9, No. 11 (1967).
6. W. H. Gust and E. B. Royce, "Axial yield strength and two successive phase transition stresses for crystalline silicon," J. Appl. Phys., 42, No. 5 (1971).
7. B. A. Graham, O. E. Jones, and J. R. Holland, "Physical behavior of germanium under shock wave compression," J. Phys. Chem. Solids, 27 (1966).
8. V. D. Urlin and A. A. Ivanov, "Melting during shock-wave compression," Dokl. Akad. Nauk SSSR, 149, No. 6 (1963).
9. N. M. Kuznetsov, "On the discontinuity of the shock adiabat during phase transitions of the first kind," Dokl. Akad. Nauk SSSR, 155, No. 1 (1964).
10. N. M. Kuznetsov, "On the shock-wave structure in the case of phase transitions of the first kind," Zh. Prikl. Mekh. Tekh. Fiz., No. 5 (1964).

11. V. D. Urlin, "Melting at ultrahigh pressures obtained in shock waves," Zh. Eksp. Teor. Fiz., 49, No. 2(8) (1965).
12. G. E. Duvall and Y. Horie, "Shock-induced phase transition," in: Proceedings of the Fourth Symposium on Detonation, Maryland (1965), pp. 248-257.
13. Y. Horie, "Melting and the Hugoniot equation," J. Phys. Chem. Solids, 28, 1569 (1967).
14. V. E. Fortov, "Hydrodynamic effects in a nonideal plasma," Teplofiz. Vys. Temp., 10, No. 1 (1972).
15. Ya. B. Zel'dovich and Yu. P. Raizer, Physics of Shock Waves and High Temperature Hydrodynamic Phenomena, Academic Press (1966-1967).
16. S. B. Kormer, "Optical investigation of characteristics of shock-compressed condensed dielectrics," Usp. Fiz. Nauk, 94, No. 4 (1968).
17. M. I. Berger, S. Joigneau, and M. G. Bottet, "Behavior of sulfur under the action of a shock wave," Compt. Rend., 250, 4331 (1960).
18. L. B. Al'tshuler, "Application of shock waves in high-pressure physics," Usp. Fiz. Nauk, 85, No. 2 (1965).
19. W. Band and G. E. Duvall, "Physical nature of shock propagation," Amer. J. Phys., 29, 780 (1961).
20. S. A. Novikov, I. I. Divnov, and A. G. Ivanov, "Investigation of the structure of compression shock waves in iron and steel," Zh. Eksp. Teor. Fiz., 47, No. 3(9) (1964).
21. R. I. Nigmatulin, "Model of motion and shock wave in two-phase solids with phase transitions," Zh. Prikl. Mekh. Tekh. Fiz., No. 1 (1970).
22. N. Kh. Akhmadeev and R. I. Nigmatulin, "Shock waves and phase transitions in iron," Zh. Prikl. Mekh. Tekh. Fiz., No. 5 (1976).
23. M. Kamegai, "Two-phase equation of state and free-energy model for dynamic phase change in materials," J. Appl. Phys., 46, No. 4 (1975).
24. J. N.Johnson, D. B. Hayes, and J. R. Assay, "Equation of state and shock-induced transformations in solid I—solid II—liquid bismuth," J. Phys. Chem. Solids, 35, 501-515 (1974).
25. G. E. Duvall, "Shock waves in solids," in: Physics of High Energy Density, New York—London (1971).
26. A. V. Anan'in, A. N. Dremin, and G. I. Kanel', "Structure of compression and rarefaction shock waves in iron," Fiz. Goreniya Vzryva, No. 1 (1972).
27. A. N. Dremin, S. V. Pershin, and V. F. Pogorelov, "Investigation of phase transitions by a magnetoelectric method," Fiz. Goreniya Vzryva, No. 4 (1965).
28. L. V. Al'tshuler, M. N. Pavlovskii, and V. P. Drakin, "Characteristics of phase transitions in compression and rarefaction shockwaves," Zh. Eksp. Teor. Fiz., 52, No. 2 (1967).
29. R. A. Graham and W. R. Brooks, "Shock wave compression of sapphire from 15 to 420 kbar. The effects of large anisotropic compressions," J. Phys. Chem. Solids, 32, 2311-2330 (1971).
30. D. P. Dandekar, "Loss of shear strength in polycrystalline tungsten under shock compression," J. Appl. Phys., 47, No. 10 (1976).
31. D. E. Grady, W. J. Murri, and G. R. Fowles, "Quartz to stishovite: wave propagation in the mixed phase region," J. Geophys. Res., 79, No. 2 (1974).
32. M. A. Podurets, G. V. Simakov, and R. F. Trunin, "On phase equilibrium in shock-compressed quartz and on the nature of the kinetics of phase transition," Fiz. Zemli, No. 7 (1976).
33. M. N. Pavlovskii and V. P. Drakin, "Problem of the metallic phase of carbon," Pis'ma, Zh. Eksp. Teor. Fiz., 4, No. 5 (1966).
34. M. A. Podurets and R. F. Trunin, "One characteristic of the shock compressibility of quartzite," Dokl. Akad. Nauk SSSR, 195, No. 4 (1970).
35. B. Alder, "Physical experiments with strong shock waves," in: Solids under High Pressure [Russian translation], Mir, Moscow (1966).
36. A. N. Dremin and O. N. Breusov, "Processes occurring in solids under the action of strong shock waves," Usp. Khim., 37, No. 5 (1968).
37. H. G. Bowden and P. M. Kelly, "The crystallography of the pressure induced phase transformation in iron alloys," Acta Metallurgy, 15, 1489-1500 (1967).
38. A. R. Kutsar and V. N. German, "The investigation of titanium structure after shock wave loading," in: Third International Conference on Titanium, Moscow (1976), p. 333.
39. Q. Johnson and A. C. Mitchell, "First x-ray diffraction evidence for a phase transition during shock-wave compression," Phys. Rev. Lett., 99, No. 20 (1972).

40. L. Kaufman and M. Cohen, "Thermodynamics and kinetics of martensite transitions," Usp. Fiz. Metallov, No. 4, 192 (1961).
41. A. Kelly and G. W. Groves, Crystallography and Crystal Defects, Addison-Wesley (1970).
42. A. L. Roitbrud, "Current state of the theory of martensite transitions," in: Investigation of Crystalline Structure and Martensite Transitions [in Russian], Nauka, Moscow (1972).
43. V. N. German, M. P. Speranskaya, L. V. Al'tshuler, and L. A. Tarasova, "Investigation of the structure of monocrystals of iron silicate deformed by strong shock waves," Fiz. Met. Metalloved., 30, No. 3, 1018 (1970).
44. H. Knapp and U. Dehlinger, "Mechanics and kinetics of diffusionless martensite transition," Acta Metallurg., 4, 289 (1956).
45. O. N. Breusov, "Phase transitions caused by shock compression," in: Proceedings of the All-Union Symposium on Pulsed Pressures [in Russian], Vol. 2, Moscow (1974), p. 18.
46. D. E. Grady, W. Y. Murry, and P. S. DeCarly, "Hugoniot sound velocities and phase transformations in two silicates," J. Geophys. Res., 80, No. 5, 4857 (1975).

SHOCK WAVES IN DILATANT AND NONDILATANT MEDIA

S. G. Artyshev and S. Z. Dunin

UDC 622.235.5+539.3+539.214

With the explosion of a charge in an isotropic brittle medium at rest and compressed by a lithostatic pressure p_h, a shock wave starts to propagate outward from the center of the explosion. A step-by-step analysis of the character of the breakdown as a function of the properties of the rock and the lithostatic pressure is given in [1-3], where the breakdown of the rock is described without taking account of the dilatant character of the behavior of the medium, i.e., without taking account of the possibility of a change in the volumetric deformation with shear [4].

The present article discusses the possibility of the propagation of a spherically symmetrical breakdown wave in dilatant and nondilatant plastic media.

The source of the breakdown wave, located in a spherical cavity (cavern) with an initial radius a_0, is a gas having an initial pressure p_{k_0}. It is assumed that the Prandtl plasticity condition is satisfied behind the front of the wave:

$$\sigma_r - \sigma_\varphi = k + m(\sigma_r + 2\sigma_\varphi), \tag{1}$$

where k and m are known constants; σ_r and σ_φ are the stresses in a radial direction and in directions orthogonal to it, respectively. The flow of the rock behind the front is described by the equations of the convservation of momentum and mass and the equation of dilatancy:

$$\rho(\partial u/\partial t + u\partial u/\partial r) = \partial\sigma_r/\partial r + 2(\sigma_r - \sigma_\varphi)/r; \tag{2}$$

$$\partial\rho/\partial t + u\partial\rho/\partial r + \rho(\partial u/\partial r + 2u/r) = 0; \tag{3}$$

$$\partial u/\partial r + 2u/r = \Lambda(\rho, \delta_r)|\partial u/\partial r - u/r|, \tag{4}$$

where ρ is the density of the medium; u is the mass velocity; r is the radius; t is the time; and $\Delta(\rho, \sigma_r)$ is the rate of dilatancy [4]. At the front of the breakdown wave, the conditions of the conservation of mass and momentum are adopted:

$$u_f(t) = \varepsilon_f(t)\dot{R}(t); \tag{5}$$

$$p_f(t) - p_h = \rho_0\varepsilon_f(t)\dot{R}^2(t), \tag{6}$$

where R(t) and $\dot{R}(t)$ are the radius and the velocity of the front; $p_h = 9.81\cdot\rho_0 h$ is the lithostatic pressure at the depth h; $\varepsilon_f = 1 - \rho_0/\rho_f$ is the discontinuity of the density at the front; and $p_f = -\sigma_f$ is the pressure at the front. Here and in what follows the subscript f denotes values of the quantities at the front, while the subscript 0 denotes values in the unperturbed medium.

Moscow. Translated from Zhurnal Prikladnoi Mekhaniki i Tekhnicheskoi Fiziki, No. 4, pp. 104-108, July-August, 1978. Original article submitted July 12, 1977.

0021-8944/78/1904-0505$07.50